Asian Journal of Chemistry; Vol. 30, No. 7 (2018), 1435-1440

ASIAN JOURNAL OF CHEMISTRY

https://doi.org/10.14233/ajchem.2018.21119

Oxidized Cellulose Fibers for Reinforment in Poly(Lactic Acid) Based Composite

F.A. SYAMANI*, Y.D. KURNIAWAN and L. SURYANEGARA

Research Center for Biomaterial, Indonesian Institute of Sciences, Jl. Raya Bogor Km. 46, Cibinong, Jawa Barat 16911, Indonesia

*Corresponding author: Fax: +62 21 87914510; Tel: +62 21 87914511; E-mail: firda.syamani@biomaterial.lipi.go.id

Received: 6 November 2017; *Accepted*: 13 April 2018; *Published online*: 31 May 2018; AJC-18909

Incompatiblity between poly(lactic acid) (PLA) and cellulose fibers due to hydrophilicity of cellulose fibers becomes the main problem in PLA-cellulose fibers composite production. Chemical modifications of cellulose fibers such as acetylation, benzoylation or acrylation have been conducted to improve the adhesion between polymer matrix and cellulose fibers. One of chemical modifications, oxidation using 2,2,6,6-tetramethylpiperidine-1-oxyl radical (TEMPO) could increase hydrophobicity of cellulose fibers without changing its fibrous morphology. However, TEMPO oxidation requires sodium bromide, HCl and chlorite that could give negative impact to the enviroment. In this study, oxidation of cellulose fibers was conducted using sodium metaperiodate (1 mol equivalent per mole of anhydroglucose unit in the cellulose) at room temperature and varied reaction time (3, 4, 5, 6 h). Subsequently, never dried the oxidized cellulose fibers were incorporated into poly(lactic acid) and gycerol triacetate to produce composite. The chemical structure changes and thermal properties of oxidized cellulose fibers were analyzed using FTIR and DSC. The mechanical properties of the resulting composite were tested using universal testing machine based on ASTM D882-75b.

Keywords: Cellulose fibers, Oxidizing, Sodium metaperiodate, Poly(lactic acid) composite.

INTRODUCTION

Cellulose fibers in the form of microfibrillated cellulose (MFC) or cellulose nanocrystal (CNC) have been studied primarily for application as fillers or reinforcement in composite materials. As "green" issue has become the main concern of many scientists, numerous applications of cellulose fibers in polymer composites such as polypropylene [1], poly(lactic acid) [2,3], poly(vinyl alcohol) [4], polyethylene [5,6], are focusing to produce "green material" with superior properties.

The main obstacle of incorporating cellulose fibers into polymer matrix is incompatibility between those two substances, which may decrease some of composite properties. Cellulose fibers are hydrophillic fibers, meanwhile some of polymer matrices show hydrophobic behavior. Some efforts had been done to overcome this barrier, such as using coupling agent or modifying cellulose fibers through chemical reaction.

Cellulose derivatives with remarkable, distinctive properties superior to the original cellulose achieved by a variety of chemical modifications, such as esterification of the cellulose with various substances: plant triglycerides [7], long chain fatty acids [8], organic acids [9] or more reactive anhydrides [10,11], which are proven to improve the cellulose hydrophobicity.

In 2006, Isogai's group in University of Tokyo has developed a new method to prepare completely individualized cellulose nanofibers 3-4 nm width and a few microns length from wood cellulose fibers by 2,2,6,6-tetramethylpiperidine-1-oxyl radical (TEMPO)-mediated oxidation under moderate aqueous condition [12]. The advantage of TEMPO-mediated oxidation on cellulose fibers is that the original fibrous morphology does not change even after oxidation with sufficient amount of reagents [13,14].

Oxidation of cellulose followed by incorporation with other functionalities is also reported [15-17]. Among these, periodate-mediated oxidation opens wider opportunity to manipulate cellulose. This approach provides a facile and significant strategy as it oxidatively cleaves the C-2 and C-3 gycol bond of the glucose ring to C-2/C-3 dialdehyde product, which is a more reactive intermediate for further derivatization [16,18]. Sirvio *et al.* [15], Rinaudo [19] and Larsson *et al.* [20] successfully prepared dialdehyde cellulose adopting this method and further improvement was achieved by Alam *et al.* [21] in salt-induced acceleration for this process. Several materials derived from this intermediate bearing distinctive properties were succesfully afforded as exemplified by highly ductile fibers prepared by subsequent reduction of the aldehyde groups by sodium borohydride [20].

In present work, we present modification of cellulose fibers (CF) isolated from oil palm empty fruit bunch (OPEFB) by regioselective oxidation using sodium metaperiodate

and utilized it as reinforcement in poly(lactic acid) based composite.

EXPERIMENTAL

Oil palm empty fruit bunch (OPEFB) from Java Island plantation was used as the source of cellulose for chemical treatment. Chemical for cellulose extraction: sodium chlorite 25 % solution, acetic acid glacial 100 %, potassium hydroxide. Chemical for oxidation: sodium chloride (NaCl), sodium meta-periodate ($NaIO_4$) and ethylene glycol. Poly(lactic acid) (PLA) semicrystalline, trade name NatureWorks™ 3001D was supplied by Cargill Dow LLC (Minnesota, USA). Glycerol triacetate (Merck) was used as plasticizer for PLA. All chemicals were used as received.

Isolation of cellulose: The 40-60 mesh oil palm empty fruit bunch biomass was subjected to a delignification process. As much as 6 g (dry basis) of air-dried OPEFB was suspended in 90 mL distilled water, then 9.6 mL sodium chlorite 25 % solution and 0.48 mL acetic acid glacial were added. The delignification process performed in waterbath at 70 °C for 1 h. After 1 h process, 9.6 mL sodium chlorite 25 % solution and 0.48 mL glacial acetic acid were again added into Erlenmeyer flask and the system was heated at 70 °C for another 1 h. This process was repeated 3 times. At the end of delignification process, the residue was filtered and washed with an excess of cold distilled water and acetone to neutrality. This residue (holocellulose) was then subsequently processed using potassium hydroxide 4 % (w/v) in the water bath at 70 °C for 2 h. The white residue, *i.e.* the resulting cellulose, was then washed until free from excess KOH and stored at -10 °C. The cellulose was obtained in 35 wt % yield calculated from the original OPEFB biomass in dry basis.

Preparation of dialdehyde cellulose fibers by oxidation reaction: Sodium chloride (1 M in overall solution) and $NaIO_4$ (1.0 mol equivalent per mole of anhydroglucose unit in the cellulose) was added to the water suspension of the cellulose fibre (fibers to water ratio of 1 g:67 mL). The beaker was completely covered with aluminium foil to avoid undesired side reaction. The mixture was stirred at 150 rpm for the desired reaction time (3, 4, 5, or 6 h) at room temperature. On the completion, ethylene glycol was added to the reaction mixture to quench the oxidation and the resulting oxidized cellulose fibers was then washed with distilled water and filtered until free from excess liquid. The oxidized cellulose fibers were then labelled according to the reaction condition, for example, S13 means the oxidation is performed using 100 mol % of $NaIO_4$ (1.0 eq.) for 3 h.

Preparation of poly(lactic acid) composite: For composite preparation, oxidized cellulose fibers in acetone were kept in a sealed container. The solid content of cellulose fibers in acetone was determined and subjected to solvent exchange process with dichlorometane. Then it was ready to be suspended gradually in dissolved PLA. As much as 1 g oxidized cellulose fibers (OCF) was added into dissolved PLA (5 g) and glycerol triacetate (1 mL) and the mixture was stirred until homogeneity for 10 min at the speed of 700 rpm. The OCF-PLA-dichloromethane mixture was spreaded on tray and the solvent was evaporated at room temperature for 12 h followed by oven drying at 60 °C for 24 h providing a sheet.

Characterization methods: The Perkin Elmer, Spectrum Two FTIR spectroscopy was used to analyze chemical structure of the oxidized cellulose fibers. The analysis was operated by an attenuated total reflection (ATR) principles, which measured the changes that occur in a totally internally reflected infrared beam when the beam came into contact with the sample. The spectral resolution was 4 cm^{-1} and the scanning range was from 4000 to 400 cm^{-1}.

DSC measurements were performed on a DSC4000 (Perkin Elmer) in the temperature ranging from 0-200 °C using approximately 5.0 mg of poly(lactic acid)-glycerol triacetate (PLA-GTA). The samples were tested at non-isothermal conditions at the heating rate of 5 °C/min. While the DSC measurement of PLA-oxidized cellulose fibers composites was conducted in the temperature range of 0-200 °C using approximately 5 mg of samples at the same heating and cooling rates of 5 °C/min in two scans: heating and cooling. The thermal properties such as glass transition temperature (T_g), cold crystallization temperature (T_{cc}), melt temperature (T_m) and enthalpy of melting (ΔH_m) were determined from the heating scan and the melt crystallization temperature (T_c) was determined from the cooling scan of the samples. The percentage of crystallinity of each sample was calculated by following equation:

$$\text{Crystallinity (\%)} = \frac{(\Delta H_m - \Delta H_c)}{\Delta H_m^{\circ}} \times 100 \quad (1)$$

In this equation, the heats of melting (ΔH_m) and cold crystallization (ΔH_{cc}) are in terms of J/g. The term ΔH_m° is a reference value and represents the heat of melting if the polymer is 100 % crystalline. The theoretically melting enthalpy of 100 % crystalline PLA was taken to be $\Delta H_m^{\circ} = 93$ J/g [22].

Tensile properties of the composite were examined based on ASTM D-882-75b standard test methods for tensile properties of thin plastic sheeting. Five specimens of composites were analyzed using a universal testing machine "Shimadzu" at a cross-head speed of 5 mm/min and a gauge length of 20 mm.

RESULTS AND DISCUSSION

In the industry, PLA can be processed in a way similar to polypropylene. However, brittleness of PLA limit the wider applications. Some plasticizer have been applied to improve PLA elongation. However, the addition of plasticizer gave negative influence on mechanical properties. Oksman *et al.* [23] used glycerol triacetate as plasticizer in compression moulded Flax/PLA composite and the result was glycerol triacetate did not improve the impact properties. Another plasticizer agent, which was poly(ethylene glycol)-PEG, also did not improve the tensile properties of the composites. Okubo [24] experimented with compression moulded bamboo fiber-reinforced PLA, adding micro-fibrillated cellulose (MFC) as an enhancer for the bending characteristics. Three point bending strength was clearly improved. They also found that tangled MFC fibers prevented micro cracks along the interface between bamboo fiber and matrix. In this study, we used glycerol triacetate (GTA) as plasticizer and oxidized cellulose fiber in PLA matrix to produce composite.

Chemical structure of oxidized cellulose: Periodate oxidation of cellulose, initially studied by Fan *et al.* [25], is a selective oxidation process that converts the 1,2-glycol groups of the glucose residues into two aldehyde groups (Fig. 1). Partial oxidation of cellulose by periodate can lead to the selective cleavage at C-2 and C-3 vicinal hydroxyl groups within glucose to yield dialdehyde units. This process can be carried out at room temperature or slightly elevated temperature [26].

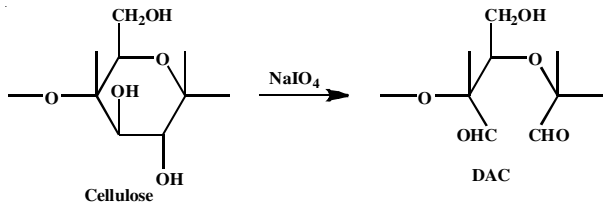

Fig. 1. Transformation of cellulose to become dialdehyde cellulose (DAC)

According to Vicini *et al.* [26], the oxidation leads to the presence of two characteristics bands of dialdehyde cellulose (DAC) in the 1720 and 880 cm^{-1} regions; they increase from a small shoulder to a distinct band increasing the oxidation levels. The broad band at 880 cm^{-1} can be assigned to the hemiacetal and hydrated form of the dialdehyde cellulose; the sharp band at 1740 cm^{-1} is characteristic of carbonyl groups streching. In addition, Fan *et al*. [25] reported that the aldehyde IR asorbance peak in periodate oxized cotton is sited in the region 1732-1734 cm^{-1} and may be attributed to the C=O streching vibration in the free aldehyde.

Fig. 2 shows IR of spectra oxidized cellulose at 3 h reaction (S13), 4 h reaction (S14), 5 h reaction (S15) and 6 h reaction (S16). The peaks of transmittance band are summarized in Table-1. Peak in 1734-1720 cm^{-1} region that were assigned to aldehyde group were not observed in all samples. In spite of this, the oxidation occured evidenced by the appearance of aldehyde groups in oxidized cellulose S13, S14 and S15, indicated by peak at 2890 cm^{-1} which was assigned to C-H strech off C=C. The highest absorbance at 2890 cm^{-1} was indicated by S15, explaining that reaction for 5 h provided more oxidized cellulose than reaction for 3 or 4 h. And 6 h reaction was not recommended because the aldehyde group tends to break.

The oxidized celulose IR spectra also showed peaks at 1628, 1633 and 1636 cm^{-1} assigned to carbonyl bond. According to Ahmed *et al.* [27], the 1632, 1640 and 1629 cm^{-1} bands are due to stretching vibration of carbonyl group characteristic of the secondary amides and other compounds containing C=O group, such as lignin. In addition, the peak at 1514 cm^{-1} implying to phenolic ring in lignin compound was not observed in all samples. Delignification using sodium chlorite at the beginning of fibers preparation and the oxidation with sodium meta-periodate has successfully removed all lignin.

Thermal analysis of PLA-GTA and modified cellulose fibers by DSC: Differential scanning calorimetry is widely used technique to determine the thermal behaviour of a material. It determines the temperature and heat flows involving phase transition in materials as a function of temperature. When the heat is absorbed from a material, the transition exhibits as endothermic peaks. If the heat is exited from material, the exothermic

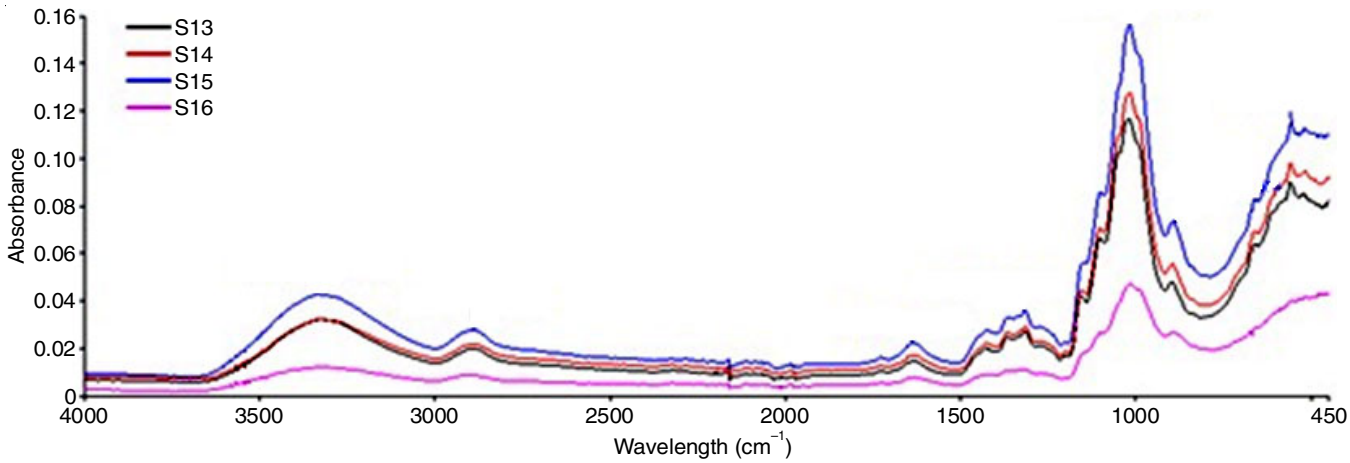

Fig. 2. FTIR spectra of oxidized cellulose fibers by 3 h reaction (S13), 4 h reaction (S14), 5 h reaction (S15) and 6 h reaction (S16)

TABLE-1
BAND CHARACTERISTICS OF FTIR SPECTRA

S13		S14		S15		S16		Assignment
Wave-number (cm^{-1})	Absorbance	Wave-number (cm^{-1})	Absorbance	Wave-number (cm^{-1})	Absorbance	Wave-number (cm^{-1})	Absorbance	
559	0.09	558	0.10	556	0.11	672	0.03	γCO at C-3, γC-C
1020	0.12	1018	0.13	1018	0.16	1015	0.15	δCOH out of plane
1316	0.03	1315	0.03	1315	0.04	1314	0.01	γCH in cellulose
1514	–	–	–	–	–	–	–	Lignin aromatic Skeleton vibration
1636	0.01	1628	0.02	1633	0.02	1634	0.01	CO (carbonyl bond)
2890	0.02	2891	0.02	2890	0.03	2891	0.01	γCH strech off CO (aldehyde group)
3329	0.03	3329	0.03	3335	0.04	3318	0.01	Streching (γ) OH (hydrogen bond)

peaks appear during the transition period [28]. Poly(lactic acid) is a slower-crystallizing material. The fastest rates of crystallization for pure PLA are found in the temperature ranges 110-130 °C, which yield spherulitic crystallization morphology [29].

As seen in Fig. 3, DSC thermogram of neat PLA 3001D showed three apparent transitions upon heating, which included PLA glass transition temperature (T_g) at 60 °C, cold crystallization temperature (T_{cc}) at 110 °C and melt temperature (T_m) at 167 °C [30]. While the DSC thermogram of PLA-GTA (Fig. 4) showed that glass transition and cold crystallization peaks were not emerged, indicating that PLA in this study was fully crystallized due to the addition of plasticizer (GTA) and heating procedure during composite production. The melting peak of PLA-GTA was shifted to lower temperature (153 °C), represented that PLA-GTA started to melt sooner than PLA. This information, will be an advantage in processing PLA-oxidized cellulose fiber composite with extruder or laboplastomill. Lower melting point indicates that less energy is required for composite processing that leads to the efficient composite cost production.

The similar pattern was appeared on DSC thermogram of PLA + GTA and its composites (Fig. 5). The heating scan, showed glass transition temperature (T_g) and melting temperature (T_m), without the peak of cold crystallization. Glass transition temperature (T_g) is influenced by amorphous structure of the sample and/or macromoleculer translation motion relative to adjacent molecules. The size of the glass transition

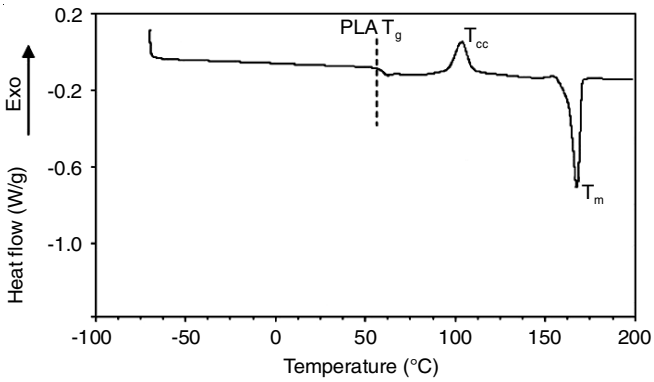

Fig. 3. DSC thermogram of PLA 3001D [Ref. 30]

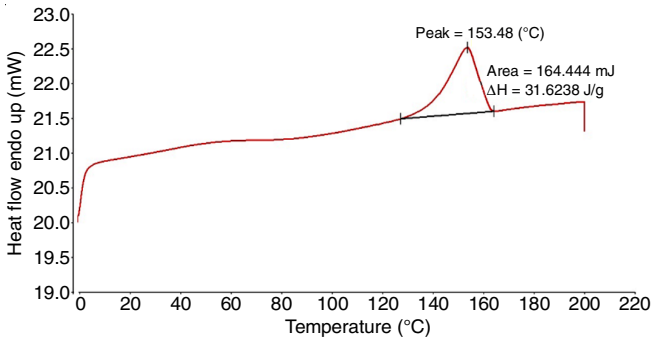

Fig. 4. DSC thermogram of PLA-glycerol triacetate

is linearly proportional to the amount of amorphous structure in the sample [31]. Amorphous and semi-crystalline polymers undergo a phase change from a glassy to rubbery stage at a glass transition temperature (T_g). At T_g the segmental mobility of molecular chains increases and a polymer is more elastic and flexible [32].

Glass transition temperature (T_g) of PLA + GTA + S13 and PLA + GTA + S14 was similar to T_g of PLA 3001D (60 ºC), which were 59.58 and 58.02 ºC, respectively. This phenomenon explained that the mobility of molecular chains in S13, S14 and PLA increased at the similar temperature, and hence altered their phase from glassy to rubbery stage. Afterward, the DSC thermogram of PLA + GTA + S15 and PLA + GTA + S16 showed that the composite's glass transition temperature was slightly higher than that of PLA. Therefore, when oxidized cellulose fibers (oxidized for 5 or 6 h) were introduced into PLA, the composites need higher temperature to change from the glassy stage to rubbery stage (Table-2).

For polymers, the glass transition is typically broader and becomes hard to measure as the crystalline content increases [31]. The temperature of glass transition (T_g) can increase or decrease with the degree of crystallinity depending on the relative density of the amorphous and crystalline states. Most often the more orderly crystalline state has the higher density at T_g and the noncrystalline molecular chains are constrained by being anchored to the immobile crystallites and T_g increases [33].

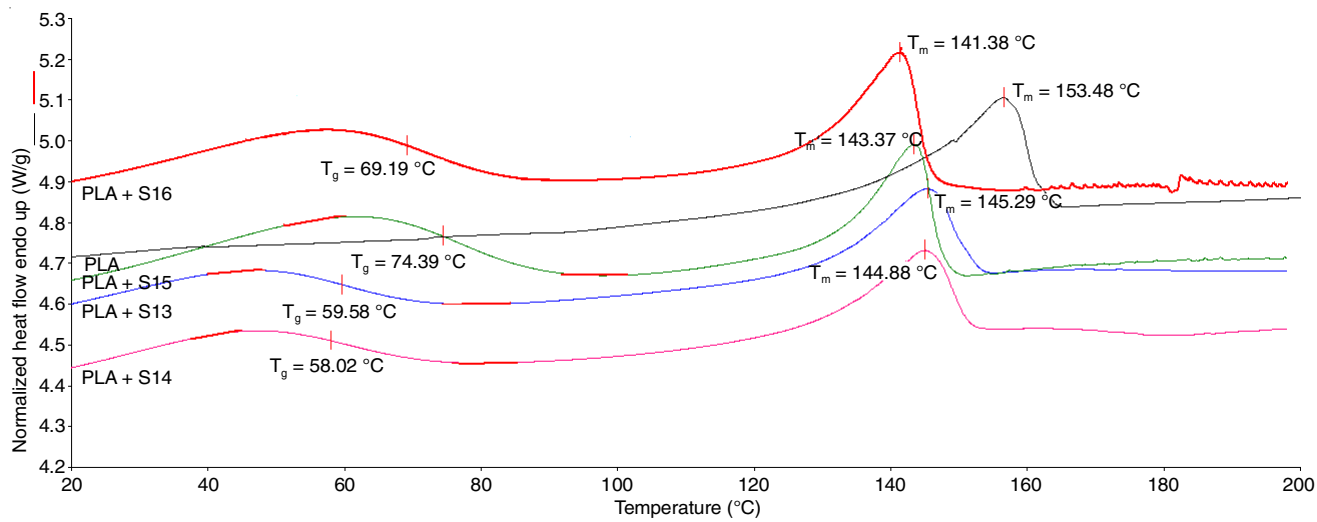

Fig. 5. DSC thermogram of oxidized cellulose fiber by 1.0 mol equivalent oxidant based on mol of anhydroglucose unit in the cellulose for 3 h (S13), 4 h (S14), 5 h (S15) and 6 h (S16) at heating scan

TABLE-2
EFFECT OF OXIDIZING TIME ON PLA-CELLULOSE COMPOSITE CRYSTALLIZATION

Samples	T_g (°C)	T_m (°C)	ΔH_m (J g^{-1})	X_c (%)
	Glass transition	Melting		Crystallinity
PLA + GTA	–	153.48	31.624	34.00
PLA + GTA + S13	59.58	145.29	40.073	43.09
PLA + GTA + S14	58.02	144.88	39.015	41.95
PLA + GTA + S15	74.39	143.37	51.209	55.06
PLA + GTA + S16	69.19	141.38	57.123	61.42

In this study, cold crystallization peak was not appeared in DSC curves of all composites, indicating that PLA was fully crystallized due to the addition of cellulose fibers and heating procedure during composite production. Therefore to calculate composite crystallinity, the melting entalphy of composite (ΔH_m) was divided by the melting entalphy of 100 % crystalline PLA (93 J/g). The addition of oxidized cellulose fibers into PLA could increase PLA crystallinity. Cellulose fibers which oxidized for 3 or 4 h produced similar composite crystallinity, 43.09 and 41.95 %, respectively. Moreover, cellulose fibers which oxidized for 5 or 6 h produced higher composite crystallinity, 55.06 and 61.42 %, respectively.

The oxidation modifies the cellulose characterization, which become more stiff and brittle. By increasing the concentration of the oxidizing agent, degree of polymerization decreases faster; therefore the methaperiodate involves a strong depolymerization of cellulose [26]. The depolymerization reaction of cellulose could disturb amorphous part of cellulose and therefore cellulose fibers become more crystalline, afterward increased the composite crystallinity.

From the DSC thermogram at cooling scan of PLA + GTA + S13 or S14 or S15 or S16 (Fig. 6), melt crystallization peaks appeared at 110.15, 104.48, 98.22, 93.90 °C, respectively. The cooling phase after melting stage, produced crystalline in all composite in this study. The higher the composite crystallinity, the lower the melt crystallization temperature.

Composite tensile properties: Representative of stress-strain curves for the composite and pure PLA are shown in Fig. 7. The addition of cellulose which were oxidized for 5 h and 6 h (S15 and S16) turned PLA composite more brittle as compared to the pure PLA as shown by the considerable decrease in the strain to failure of the composites. The strain to failure decreased from 13.5 % for the pure PLA to 9.4 % for the PLA + S15 composite and 5.6 % for the PLA+S16 composite. Meanwhile the addition of cellulose which was oxidized for 3 h and 4 h (S13 and S14) did not give significant influence to the PLA strain.

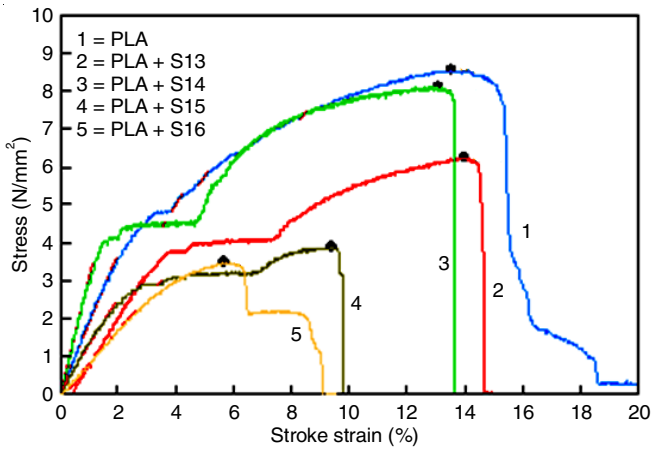

Fig. 7. Stress-Strain curves of PLA, PLA + oxidized cellulose fibre (S13, S14, S15 or S16)

The strain to failure of the PLA + S13 and PLA S14 was higher than that of the PLA + S15 and PLA + S16, implying greater toughness. Moreover, the tensile strength of PLA + S14 (Fig. 8) was the highest among those of other composites in this study. This superior mechanical properties were probably as a result of the more compact composite structure, so that the stress could be transferred equally to all composite element.

Bulota *et al.* [34] used Raman spectroscopy to investigate deformation mechanism of TEMPO-oxidizedfibrillated cellu-

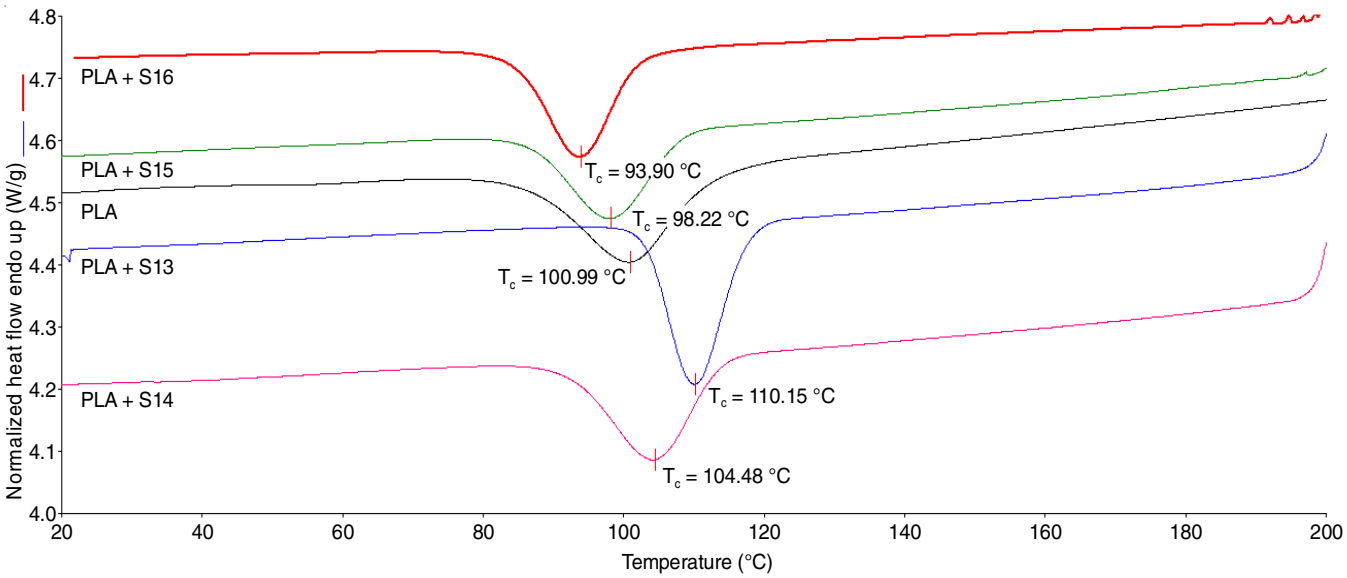

Fig. 6. DSC thermogram of oxidized cellulose fiber by 1.0 mol equivalent oxidant based on mol of anhydroglucose unit in the cellulose for 3 h (S13), 4 h (S14), 5 h (S15) and 6 h (S16) at cooling scan

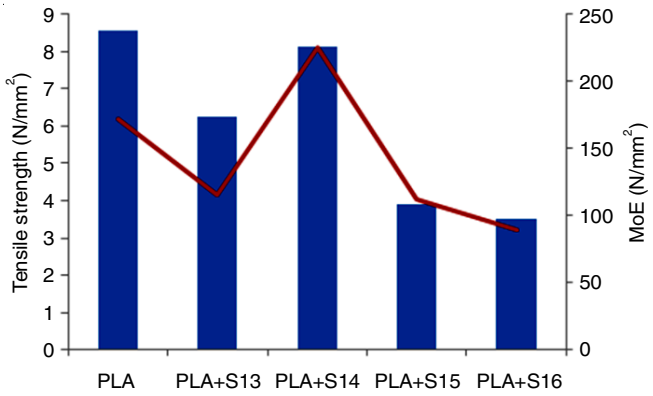

Fig. 8. Tensile strength and modulus of PLA, PLA + oxidized cellulose (S13, S14, S15 or S16)

lose (TOFC)-reinforced composite, finding that stress trasfer became dominated by the network mechanics at 30 wt % loading of TOFC.

ACKNOWLEDGEMENTS

The authors are grateful to Research Center for Biomaterial-Indonesian Institute of Sciences (SP DIPA-079.01.2.649132/2017), Government of Indonesia in conjunction with JST-JICA-SATREPS Biorefinery Program Research-2017.

REFERENCES

1. S.H. Lee, S. Wang, G.M. Pharr and H. Xu, *Composites Part A*, **38**, 1517 (2007); https://doi.org/10.1016/j.compositesa.2007.01.007.
2. A.N. Nakagaito, A. Fujimura, T. Sakai, Y. Hama and H. Yano, *Compos. Sci. Technol.*, **69**, 1293 (2009); https://doi.org/10.1016/j.compscitech.2009.03.004.
3. L. Suryanegara, A.N. Nakagaito and H. Yano, *Compos. Sci. Technol.*, **69**, 1187 (2009); https://doi.org/10.1016/j.compscitech.2009.02.022.
4. M.S. Peresin, Y. Habibi, J.O. Zoppe, J.J. Pawlak and O.J. Rojas, *Biomacromolecules*, **11**, 674 (2010); https://doi.org/10.1021/bm901254n.
5. A. Sdrobis, R.N. Darie, M. Totolin, G. Cazacu and C. Vasile, *Composites Part B*, **43**, 1873 (2012); https://doi.org/10.1016/j.compositesb.2012.01.064.
6. R. Chollakup, W. Smitthipong, W. Kongtud and R. Tantatherdtam, *J. Adhes. Sci. Technol.*, **27**, 1290 (2013); https://doi.org/10.1080/01694243.2012.694275.
7. T.A. Dankovich and Y.L. Hsieh, *Cellulose*, **14**, 469 (2007); https://doi.org/10.1007/s10570-007-9132-1.
8. P. Uschanov, L.S. Johansson, S.L. Maunu and J. Laine, *Cellulose*, **18**, 393 (2011); https://doi.org/10.1007/s10570-010-9478-7.
9. K.Y. Lee, F. Quero, J.J. Blaker, C.A.S. Hill, S.J. Eichhorn and A. Bismarck, *Cellulose*, **18**, 595 (2011); https://doi.org/10.1007/s10570-011-9525-z.
10. W.J. Wang, W.W. Wang and Z.Q. Shao, *Cellulose*, **21**, 2529 (2014); https://doi.org/10.1007/s10570-014-0295-2.
11. S.S. Eyley and W. Thielemans, *Nanoscale*, **6**, 7764 (2014); https://doi.org/10.1039/C4NR01756K.
12. H. Fukuzumi, Ph.D. Thesis, Studies on Structures and Properties of TEMPO-oxidized Cellulose Nanofibril Films, Thesis, Departement of Biomaterial Sciences, Graduate School of Agricultural and Life Sciences, The University of Tokyo, Japan (2012).
13. T. Saito, S. Kimura, Y. Nishiyama and A. Isogai, *Biomacromolecules*, **8**, 2485 (2007); https://doi.org/10.1021/bm0703970.
14. T. Saito, M. Hirota, N. Tamura, S. Kimura, H. Fukuzumi, L. Heux and A. Isogai, *Biomacromolecules*, **10**, 1992 (2009); https://doi.org/10.1021/bm900414t.
15. J. Sirvio, H. Liimatainen, J. Niinimäki and O. Hormi, *Carbohydr. Polym.*, **86**, 260 (2011); https://doi.org/10.1016/j.carbpol.2011.04.054.
16. R. Dash, T. Elder and A.J. Ragauskas, *Cellulose*, **19**, 2069 (2012); https://doi.org/10.1007/s10570-012-9769-2.
17. E. Loranger, A.O. Piché and C. Daneault, *Nanomaterials*, **2**, 286 (2012); https://doi.org/10.3390/nano2030286.
18. I. Paterson, K.K.H. Ng, S. Williams, D.C. Millican and S.M. Dalby, *Angew. Chem.*, **53**, 2692 (2014); https://doi.org/10.1002/anie.201310164.
19. M. Rinaudo, *Polymers*, **2**, 505 (2010); https://doi.org/10.3390/polym2040505.
20. P.A. Larsson, L.A. Berglund and L. Wagberg, *Cellulose*, **21**, 323 (2014); https://doi.org/10.1007/s10570-013-0099-9.
21. M.N. Alam, M. Antal, A. Tejado and T.G.M. van de Ven, *Cellulose*, **19**, 517 (2012); https://doi.org/10.1007/s10570-011-9649-1.
22. M. Pyda and B. Wunderlich, *Macromolecules*, **38**, 10472 (2005); https://doi.org/10.1021/ma051611k.
23. K. Oksman, M. Skrifvars and J.F. Selin, *Compos. Sci. Technol.*, **63**, 1317 (2003); https://doi.org/10.1016/S0266-3538(03)00103-9.
24. K. Okubo, T. Fujii and N. Yamashita, *JSME Int. J. Ser. A.*, **48**, 199 (2005); https://doi.org/10.1299/jsmea.48.199.
25. Q.G. Fan, D.M. Lewis and K.N. Tapley, *J. Appl. Polym. Sci.*, **82**, 1195 (2001); https://doi.org/10.1002/app.1953.
26. S. Vicini, E. Princi, G. Luciano, E. Franceschi, E. Pedemonte, D. Oldak, H. Kaczmarek and A. Sionkowska, *Thermochim. Acta*, **418**, 123 (2004); https://doi.org/10.1016/j.tca.2003.11.049.
27. K.K.M. Ahmed, A.C. Rana and V.K. Dixit, *Pharmacogn. Mag.*, **1**, 48 (2005).
28. S.C. Mojumdar, M. Sain, R.C. Prasad, L. Sun and J.E.S. Venart, *J. Therm. Anal. Calorim.*, **90**, 653 (2007); https://doi.org/10.1007/s10973-007-8518-5.
29. D. Garlotta, *J. Polym. Environ.*, **9**, 63 (2001); https://doi.org/10.1023/A:1020200822435.
30. K.A. Afrifah and L.M. Matuana, *Macromol. Mater. Eng.*, **295**, 802 (2010); https://doi.org/10.1002/mame.201000107.
31. W.M. Groenewoud, Differential Scanning Calorimetry, In: Characteriztion of Polymeric Materials by Thermal Analysis, Elsevier Science B.V., Chap. 1, pp. 10-60 (2001).
32. A. Gregorova, ed.: A.A. Elkordy, Application of Differential Scanning Calorimetry to the Characterization of Biopolymers, Applications of Calorimetry in a Wide Context-Differential Scanning Calorimetry, Isothermal Titration Calorimetry and Microcalorimetry, InTech, Chap. 1 (2013).
33. M.M. Rahman, S. Afrin, P. Haque, M.M. Islam, M.S. Islam and M.A. Gafur, *Int. J. Chem. Eng.*, **2014**, 1 (2014); https://doi.org/10.1155/2014/842147.
34. M. Bulota, S. Tanpichai, M. Hughes and S.J. Eichhorn, *ACS Appl. Mater. Interfaces*, **4**, 331 (2012); https://doi.org/10.1021/am201399q.